Wireless caching helper networks : ginibre point process modeling and analysis

Kong, Han-Bae; Flint, Ian; Wang, Ping; Niyato, Dusit; Privault, Nicolas

2018

Kong, H.-B., Flint, I., Wang, P., Niyato, D., & Privault, N. (2018). Wireless caching helper networks : ginibre point process modeling and analysis. Proceedings of 2018 IEEE International Conference on Communications (ICC). doi:10.1109/ICC.2018.8422493

https://hdl.handle.net/10356/137247

https://doi.org/10.1109/ICC.2018.8422493

Wireless Caching Helper Networks: Ginibre Point Process Modeling and Analysis

Han-Bae Kong, Ian Flint, Ping Wang, Dusit Niyato, and Nicolas Privault

***Abstract*—In this paper, we consider wireless caching helper networks (WCHNs) consisting of cache-enabled device-to-device (D2D) transmitters and caching helpers (CHs), which deliver data by exploiting cached contents. We consider two types of modes at a typical user, namely D2D and CH modes. In the D2D and CH modes, after requesting a content, the user receives the content from a D2D transmitter and a CH caching the content, respectively. In practical scenarios, to mitigate interference, the CHs may not be placed close to each other, and thus there exists a form of repulsion among the CHs' locations. In this context, we model the spatial distribution of the CHs as a β-Ginibre point processe, which reflects the repulsive behavior and contains the Poisson point process as a special case. Then, we provide analytical expressions for the coverage probabilities in the WCHNs.**

***Index Terms*—Wireless caching helper networks, edge caching, device-to-device communications, repulsive point process, Ginibre point process, stochastic geometry.**

I. Introduction

It was reported in [1] that an exponential growth of mobile data traffic is mainly driven by on-demand video streaming. Delivering large volume of data from content providers to end users incurs traffic congestion in backhaul links, which results in slow transmission rate and high latency. As a means to alleviate the congestion, caching popular contents at the edge of the networks has generated significant interest [2]. The authors in [3] studied the content placement problem in a wireless network consisting of caching helpers and wireless users. In [4], both deterministic caching and random caching strategies for a wireless device-to-device (D2D) caching network were proposed.

The performance of caching wireless networks was investigated in [5]–[9]. The work in [5] and [6] analyzed the outage probability of cache-enabled small-cell networks with/without underlying macro cellular network, respectively, when the locations of nodes in the networks are assumed to be distributed as Poisson point processes (PPPs). Additionally, the coverage probability of cache-enabled D2D networks was characterized by modeling the spatial distribution of the devices as a PPP [7]. The authors in [8] and [9] investigated the performance of wireless caching helper networks (WCHNs) consisting of a number of caching helpers whose locations are modeled by a PPP.

In practical networks, in order to alleviate interference or increase coverage area, transmitters in wireless networks may not be placed close to each other, and hence there exists repulsion among the locations of the transmitters [10]. In this context, Ginibre point processes (GPPs) [11] which take the repulsive nature into account, have been successfully adopted as the models for various wireless networks [12]–[15]. The α-GPP ($-1 \leq \alpha < 0$) is a superposition of $-1/\alpha$ independent GPPs [16]. With the α-GPP model, the authors in [12] and [13] provided analytical expressions for the performance of wireless sensor networks with/without a fractional channel inversion power control, respectively. Another kind of parameterization of the GPP is the so-called β-GPP ($0 < \beta \leq 1$) which is a thinned and re-scaled GPP, generated by retaining each point of the GPP independently with probability β [17]. Exploiting the specificities of the β-GPP, the coverage probabilities in single-tier and heterogeneous cellular networks were analyzed in [14] and [15], respectively.

It should be remarked that the previous works on WCHNs in [8] and [9] assumed that the locations of CHs follow a PPP due to its analytical simplicity. Despite the fact that CHs in practical WCHNs may experience a repulsive nature, the performance of the WCHNs, which takes the repulsion into account has not been studied yet.

In this paper, we analyze the coverage probability of the WCHNs consisting of cache-enabled D2D transmitters and CHs by modeling the spatial distributions of the CHs and the D2D transmitters as a β-GPP and a PPP, respectively.

Two types of user access modes are considered when a typical user requests a content, namely D2D and CH modes. In the D2D (respectively CH) mode, the typical user is associated with the closest D2D transmitter (respectively CH) which caches the requested content and is within a certain distance. Unlike what happens in the PPP setting, when the locations of the CHs follow a β-GPP, the interferences from the CHs are correlated. We obtain analytical expressions for the coverage probabilities in the D2D and the CHs modes by accounting for the correlation. For the β-GPP, the parameter β presents the degree of the repulsion, and the β-GPP weakly converges to the PPP as $\beta \to 0$. Motivated by this fact, we derive analytical results in the PPP by letting $\beta \to 0$ in our general results.

Throughout the paper, we use the following notations. $\mathbb{P}(A)$ and $\mathbb{E}[X]$ represent the probability of an event A and the expectation of a random variable X, respectively. The notations $\|\mathbf{x}\|$, $|x|$ and x^* stand for the Euclidean 2-norm of $\mathbf{x}$, Euclidean norm and conjugate of a complex scalar x, respectively. Lastly, $\Phi \sim PPP(\lambda)$ and $\Phi \sim GPP(\lambda, \beta)$ mean that a point process Φ follows a PPP with intensity λ and a β-GPP with intensity λ and repulsion parameter β, respectively.

II. System Model and Preliminaries

A. Network model

In this paper, we investigate WCHNs comprising of cache-enabled D2D transmitters and CHs, which are equipped with

H.-B. Kong, P. Wang and D. Niyato are with the School of Computer Science and Engineering, Nanyang Technological University, Singapore 639798 (e-mail: hbkong@ntu.edu.sg; wangping@ntu.edu.sg; dniyato@ntu.edu.sg). I. Flint and N. Privault are with the School of Physical and Mathematical Sciences, Nanyang Technological University, Singapore 639798 (e-mail: iflint@ntu.edu.sg; nprivault@ntu.edu.sg).

This work was supported in part by Singapore MOE Tier 1 (2017-T1-002-007 and RG33/16), MOE Tier 2 (MOE2014-T2-2-015 ARC4/15 and MOE2016-T2-1-036) and NRF2015-NRF-ISF001-2277.

caching storage units. As explained previously, we consider two types of user access modes for a typical user requesting a content c, namely D2D and CH modes. In the D2D (or CH) mode, the user is connected to the nearest D2D transmitter (or CH) which stores the content c and is within the distance r_D (or r_H). Here, r_D and r_H represent the maximum distances in the D2D and the CH modes, respectively.

In order to take into account the repulsive nature in practical networks [10], we model the spatial distribution of the CHs by a β-GPP Φ_H with repulsion parameter β_H and intensity λ_H. Also, the locations of the D2D transmitters are assumed to follow a PPP with intensity λ_D, as the locations of the D2D users are typically independent.

B. Caching

Let us define a finite content category $\mathcal{C} = \{c_1, c_2, \ldots, c_M\}$ where c_m is the m-th most popular content for $m = 1, \ldots, M$. It is assumed that all contents have the same size, which is normalized to one [5]. We assume that each D2D transmitter and each CH has a cache storage of sizes s_D and s_H, respectively. Let us denote by η_{D_m} and η_{H_m} the probabilities that a content $c_m \in \mathcal{C}$ is cached at a D2D transmitter and a CH, respectively.

We consider two types of pre-fetching strategies called *random caching strategy (RCS)* and *popularity-based caching strategy (PCS)*. For the RCS, each node randomly caches files regardless of their popularity, and thus $\eta_{D_m} = s_D/M$ and $\eta_{H_m} = s_H/M$. For the PCS, each D2D transmitter and each CH proactively store the s_D and s_H most popular files, respectively. Hence, we have $\eta_{D_m} = 1$ if $m \leq s_D$ and $\eta_{D_m} = 0$ otherwise. Also, $\eta_{H_m} = 1$ if $m \leq s_H$ and $\eta_{H_m} = 1$ otherwise.

Since each D2D transmitter caches contents independently from other D2D transmitters, for a given content c_m, the D2D transmitters can be divided into two groups, namely the D2D transmitters which cache c_m (Φ_{D_m}) and the D2D transmitters which do not ($\tilde{\Phi}_{D_m}$) where $\Phi_{D_m} \cup \tilde{\Phi}_{D_m} = \Phi_D$. In a similar fashion, the spatial distribution of the CHs which have c_m, and the locations of the CHs which do not, are respectively defined as Φ_{H_m} and $\tilde{\Phi}_{H_m}$ where $\Phi_{H_m} \cup \tilde{\Phi}_{H_m} = \Phi_H$. Then, the intensities of Φ_{D_m}, $\tilde{\Phi}_{D_m}$, Φ_{H_m} and $\tilde{\Phi}_{H_m}$ are equal to $\eta_{D_m}\lambda_D$, $(1-\eta_{D_m})\lambda_D$, $\eta_{H_m}\lambda_H$ and $(1-\eta_{H_m})\lambda_H$, respectively.

It is assumed that the content popularity follows the Zipf distribution [18], and therefore the probability that the m-th most popular content c_m is requested is given by

$$\xi_m = \frac{1}{m^\delta}\left(\sum_{j=1}^{M}\frac{1}{j^\delta}\right)^{-1}. \tag{1}$$

Note that the lower indexed content has a higher popularity, i.e., $\xi_i > \xi_j$ if $i < j$. Here, $\delta(\geq 0)$ models the skewness of the popularity profile.

C. Signal-to-interference ratio (SIR)

Thanks to the stationarity of the β-GPP [17], without loss of generality, we assume that the typical user is located at the origin o. First, let us focus on the D2D mode. When the user requests the content c_m and the user is connected to the nearest D2D transmitter in Φ_{D_m}, we express the SIR γ_{D_m} as

$$\gamma_{D_m} = \frac{P_D h_{D_{m,o}} \|\mathbf{x}_{D_{m,o}}\|^{-\alpha}}{I_{D_m} + I_H}, \tag{2}$$

where

$$D_{m,o} = \underset{i\in\mathbb{N}\text{ s.t. }\mathbf{x}_i\in\Phi_{D_m}}{\arg\min} \|\mathbf{x}_i\|,$$

$$I_H = \sum_{k\in\mathbb{N}\text{ s.t. }\mathbf{x}_k\in\Phi_H} P_H g_k \|\mathbf{x}_k\|^{-\alpha}, \tag{3}$$

$$I_{D_m} = \hat{I}_{D_m} + \tilde{I}_{D_m}, \tag{4}$$

$$\hat{I}_{D_m} \triangleq \sum_{k\in\mathbb{N}\setminus\{D_{m,o}\}\text{ s.t. }\mathbf{x}_k\in\Phi_{D_m}} P_D h_k \|\mathbf{x}_k\|^{-\alpha},$$

$$\tilde{I}_{D_m} \triangleq \sum_{k\in\mathbb{N}\text{ s.t. }\mathbf{x}_k\in\tilde{\Phi}_{D_m}} P_D h_k \|\mathbf{x}_k\|^{-\alpha},$$

where P_D and P_H represent the transmit powers at the D2D transmitters and the CHs, respectively. Here, α and h_k denote the path loss exponent and the gain of the small-scale fading channel between the user and the D2D transmitter located at $\mathbf{x}_k$, and g_k indicates the gain of the small-scale fading channel between the user and the CH located at $\mathbf{x}_k$.

Next, for the CH mode, when the user accesses the content c_m and receives the content from the closest CH in Φ_{H_m}, the SIR γ_{H_m} is written as

$$\gamma_{H_m} = \frac{P_H g_{H_{m,o}} \|\mathbf{x}_{H_{m,o}}\|^{-\alpha}}{I_D + I_{H_m}}, \tag{5}$$

where

$$H_{m,o} = \underset{i\in\mathbb{N}\text{ s.t. }\mathbf{x}_i\in\Phi_{H_m}}{\arg\min} \|\mathbf{x}_i\|,$$

$$I_D = \sum_{k\in\mathbb{N}\text{ s.t. }\mathbf{x}_k\in\Phi_D} P_D h_k \|\mathbf{x}_k\|^{-\alpha}, \tag{6}$$

$$I_{H_m} = \hat{I}_{H_m} + \tilde{I}_{H_m}, \tag{7}$$

$$\hat{I}_{H_m} \triangleq \sum_{k\in\mathbb{N}\setminus\{H_{m,o}\}\text{ s.t. }\mathbf{x}_k\in\Phi_{H_m}} P_H g_k \|\mathbf{x}_k\|^{-\alpha},$$

$$\tilde{I}_{H_m} \triangleq \sum_{k\in\mathbb{N}\text{ s.t. }\mathbf{x}_k\in\tilde{\Phi}_{H_m}} P_H g_k \|\mathbf{x}_k\|^{-\alpha}.$$

D. Coverage Probability

We define the coverage probability as the probability that the SIR is larger than a pre-defined SIR threshold γ_{th}. Then, the coverage probabilities for the two modes are respectively equal to

$$\mathcal{P}_{D_m} \triangleq \mathbb{P}\left(\gamma_{D_m} \geq \gamma_{th}, \|\mathbf{x}_{D_{m,o}}\| \leq r_D\right), \tag{8}$$

$$\mathcal{P}_{H_m} \triangleq \mathbb{P}\left(\gamma_{H_m} \geq \gamma_{th}, \|\mathbf{x}_{H_{m,o}}\| \leq r_H\right). \tag{9}$$

When the typical user operates in the D2D mode or the CH mode, the average coverage probabilities $\mathcal{P}_{D,cov}$ and $\mathcal{P}_{H,cov}$ are respectively given by

$$\mathcal{P}_{D,cov} = \sum_{m=1}^{M} \xi_m \mathcal{P}_{D_m}, \tag{10}$$

$$\mathcal{P}_{H,cov} = \sum_{m=1}^{M} \xi_m \mathcal{P}_{H_m}. \tag{11}$$

E. Preliminaries

Let us consider the β-GPP $\Phi = \{\mathbf{x}_k\}_{k\in\mathbb{N}}$ with intensity λ and repulsion parameter β. Then, the set $\{\|\mathbf{x}_k\|^2\}_{k\in\mathbb{N}}$ has the same distribution as the set χ constructed from an i.i.d. sequence $\{B_i\}_{i\in\mathbb{N}}$ by deleting each B_i independently and with probability $1-\beta$ where $B_i \sim \mathcal{G}\left(i, \beta/(\pi\lambda)\right)$ and $\mathcal{G}(a,b)$ denotes a gamma random variable with shape parameter a and scale parameter b [17].

In this model, the received signal at the user from the CH at $\mathbf{x}_k$ becomes $P_H g_k \|\mathbf{x}_k\|^{-\alpha} = P_H g_k B_{H,k}^{-\alpha/2}$ where

$B_{H,k} \sim \mathcal{G}(k, \beta_H/(\pi\lambda_H))$. In addition, the sum of the received signals at the user from the CHs is expressed as $\sum_{\mathbf{x}_k \in \Phi_H} P_H g_k \|\mathbf{x}_k\|^{-\alpha} = \sum_{k=1}^{\infty} P_H g_k B_{H,k}^{-\alpha/2} \Xi_{H,k}$ where $\{\Xi_{H,k}\}$ indicates a set of independent discrete random variables with $\mathbb{E}[\Xi_{H,k}] = \beta_H$ and $\Xi_{H,k} \in \{0,1\}$. Here, the probability density function (PDF) of $B_{H,k}$ is given by

$$f_{B_{H,k}}(x) = \frac{x^{k-1}}{\left(\frac{\beta_H}{\pi\lambda_H}\right)^k \Gamma(k)} \exp\left(-\frac{\pi\lambda_H}{\beta_H} x\right). \quad (12)$$

Before analyzing the coverage probability, let us derive the Laplace transforms which are utilized in Section III. We denote the Laplace transform of a random variable X by $\mathcal{L}_X(s) \triangleq \mathbb{E}[\exp(-sX)]$. Then, the Laplace transforms of I_H and I_D in (3) and (6) are respectively derived as [19]

$$\begin{aligned}\mathcal{L}_{I_H}(s) &= \mathbb{E}\left[\prod_{k=1}^{\infty} \exp\left(-sP_H g_k B_{H,k}^{-\alpha/2} \Xi_{H,k}\right)\right] \quad (13)\\ &= \mathbb{E}\left[\prod_{k=1}^{\infty} \frac{1}{1 + sP_H B_{H,k}^{-\alpha/2} \Xi_{H,k}}\right]\\ &= \mathbb{E}\left[\prod_{k=1}^{\infty} \left(\frac{\beta_H}{1 + sP_H B_{H,k}^{-\alpha/2}} + 1 - \beta_H\right)\right]\\ &= \prod_{k=1}^{\infty} \left(\int_0^{\infty} \frac{\beta_H}{1 + sP_H x^{-\alpha/2}} f_{B_{H,k}}(x)\,\mathrm{d}x + 1 - \beta_H\right),\end{aligned}$$

$$\mathcal{L}_{I_D}(s) = \exp\left(-\frac{2\pi^2\lambda_D}{\alpha \sin\left(\frac{2\pi}{\alpha}\right)} (sP_D)^{2/\alpha}\right). \quad (14)$$

Now, we introduce the distributions of the contact distances $\|\mathbf{x}_{H_{m,o}}\|$ and $\|\mathbf{x}_{D_{m,o}}\|$. The cumulative distribution functions (CDFs) of $\|\mathbf{x}_{H_{m,o}}\|$ and $\|\mathbf{x}_{D_{m,o}}\|$ are identified as

$$\begin{aligned}F_{\|\mathbf{x}_{H_{m,o}}\|}(x) &= \mathbb{P}\left(\|\mathbf{x}_{H_{m,o}}\| \le x\right) \quad (15)\\ &= 1 - \mathbb{P}\left(\forall \mathbf{x}_i \in \Phi_{H_m}, \|\mathbf{x}_i\| > x\right)\\ &= 1 - \prod_{k=1}^{\infty} \left(\eta_{H_m}\beta_H \mathbb{P}\left(B_{H,k} > x^2\right) + 1 - \eta_{H_m}\beta_H\right)\\ &= 1 - \prod_{k=1}^{\infty} \left(1 - \frac{\eta_{H_m}\beta_H}{\Gamma(k)} \gamma\left(k, \frac{\pi\lambda_H}{\beta_H} x^2\right)\right),\end{aligned}$$

$$F_{\|\mathbf{x}_{D_{m,o}}\|}(x) = 1 - \exp\left(-\pi\eta_{D_m}\lambda_D x^2\right), \quad (16)$$

where $\gamma(a,b) = \int_0^b t^{a-1}e^{-t}\,\mathrm{d}t$ is the lower-incomplete gamma function.

In addition, when $\Phi_H \sim PPP(\lambda_H)$, the Laplace transform of I_{H_m} in (7) is computed as

$$\begin{aligned}&\mathcal{L}_{I_{H_m}}(s, \|\mathbf{x}_{H_{m,o}}\|) = \mathcal{L}_{\hat{I}_{H_m}}(s, \|\mathbf{x}_{H_{m,o}}\|)\mathcal{L}_{\tilde{I}_{H_m}}(s), \quad (17)\\ &\mathcal{L}_{\hat{I}_{H_m}}(s, \|\mathbf{x}_{H_{m,o}}\|)\\ &= \exp\left(-2\pi\eta_{H_m}\lambda_H \int_{\|\mathbf{x}_{H_{m,o}}\|}^{\infty} \frac{x}{1 + x^{\alpha}/(sP_H)}\,\mathrm{d}x\right),\\ &\mathcal{L}_{\tilde{I}_{H_m}}(s) = \exp\left(-\frac{2\pi^2(1-\eta_{H_m})\lambda_H}{\alpha \sin\left(\frac{2\pi}{\alpha}\right)} (sP_H)^{2/\alpha}\right).\end{aligned}$$

Similarly to (17), the Laplace transform of I_{D_m} in (4) becomes

$$\begin{aligned}&\mathcal{L}_{I_{D_m}}(s, \|\mathbf{x}_{D_{m,o}}\|) = \mathcal{L}_{\hat{I}_{D_m}}(s, \|\mathbf{x}_{D_{m,o}}\|)\mathcal{L}_{\tilde{I}_{D_m}}(s), \quad (18)\\ &\mathcal{L}_{\hat{I}_{D_m}}(s, \|\mathbf{x}_{D_{m,o}}\|)\\ &= \exp\left(-2\pi\eta_{D_m}\lambda_D \int_{\|\mathbf{x}_{D_{m,o}}\|}^{\infty} \frac{x}{1 + x^{\alpha}/(sP_D)}\,\mathrm{d}x\right),\end{aligned}$$

$$\mathcal{L}_{\tilde{I}_{D_m}}(s) = \exp\left(-\frac{2\pi^2(1-\eta_{D_m})\lambda_D}{\alpha \sin\left(\frac{2\pi}{\alpha}\right)} (sP_D)^{2/\alpha}\right).$$

III. Performance Analysis

In this section, we introduce expressions for the coverage probabilities in Section II-D.

A. CH mode

When the user is connected to the closest CH located at $\mathbf{x}_{H_{m,o}}$, the SIR γ_{H_m} in (5) is written as

$$\gamma_{H_m} = \frac{P_H g_{H_{m,o}} B_{H,H_{m,o}}^{-\alpha/2}}{I_D + \sum_{k \in \mathbb{N}\setminus\{H_{m,o}\}} P_H g_k B_{H,k}^{-\alpha/2} \Xi_{H,k}}. \quad (19)$$

We derive an expression for the coverage probability $\mathcal{P}_{H_m}$ in the following theorem.

Theorem 1. *When the typical user requesting the content c_m operates in the CH mode, the coverage probability $\mathcal{P}_{H_m}$ in* (9) *is written as*

$$\begin{aligned}\mathcal{P}_{H_m} = 2\pi\eta_{H_m}\lambda_H \int_0^{r_H} &\mathcal{L}_{I_D}\left(\frac{\gamma_{th} z^{\alpha}}{P_H}\right) \exp\left(-\frac{\pi\lambda_H z^2}{\beta_H}\right)\\ &\times \Upsilon_{H_m}\left(\frac{\pi\lambda_H z^2}{\beta_H}\right) \Delta_{H_m}\left(\frac{\pi\lambda_H z^2}{\beta_H}\right) z\,\mathrm{d}z, \quad (20)\end{aligned}$$

where $\mathcal{L}_{I_D}(s)$ is defined in (14) *and for any $x > 0$ we set*

$$\Upsilon_{H_m}(x) = \sum_{i=1}^{\infty} \frac{x^{i-1}}{\Gamma(i)} \left(A_{\eta_{H_m},\beta_{H,i}}(x, \gamma_{th} x^{\alpha/2})\right)^{-1}, \quad (21)$$

$$\Delta_{H_m}(x) = \prod_{k=1}^{\infty} A_{\eta_{H_m},\beta_{H,k}}(x, \gamma_{th} x^{\alpha/2}), \quad (22)$$

$$\begin{aligned}A_{n,b,k}(x,\tau) = 1 - b &+ \int_x^{\infty} \frac{nb\nu^{k-1}\exp(-\nu)}{\Gamma(k)\left(1 + \tau\nu^{-\alpha/2}\right)}\,\mathrm{d}\nu \quad (23)\\ &+ \int_0^{\infty} \frac{(1-n)b\nu^{k-1}\exp(-\nu)}{\Gamma(k)\left(1 + \tau\nu^{-\alpha/2}\right)}\,\mathrm{d}\nu.\end{aligned}$$

Proof. See Appendix A. □

When $\Phi_H \sim PPP(\lambda_H)$, we obtain an expression for the coverage probability $\mathcal{P}_{H_m}$ by letting $\beta_H \to 0$, as presented in the following theorem.

Theorem 2. *When $\Phi_H \sim PPP(\lambda_H)$, the coverage probability $\mathcal{P}_{H_m}$ in* (9) *is expressed as*

$$\mathcal{P}_{H_m} = \int_0^{r_H} \mathcal{L}_{I_{H_m}}\left(\frac{\gamma_{th} z^{\alpha}}{P_H}, z\right) \mathcal{L}_{I_D}\left(\frac{\gamma_{th} z^{\alpha}}{P_H}\right) f_{\|\mathbf{x}_{H_{m,o}}\|}(z)\,\mathrm{d}z, \quad (24)$$

$$f_{\|\mathbf{x}_{H_{m,o}}\|}(x) = 2\pi\eta_{H_m}\lambda_H x \exp\left(-\pi\eta_{H_m}\lambda_H x^2\right),$$

where $\mathcal{L}_{I_{H_m}}$ and $\mathcal{L}_{I_D}$ are defined in (17) *and* (14)*, respectively.*

Proof. See Appendix B. □

B. D2D mode

When the user requests the content c_m and it is associated with the nearest D2D transmitter which has the content c_m, we rewrite the SIR γ_{D_m} in (2) as

$$\gamma_{D_m} = \frac{P_D h_{D_{m,o}} B_{D,D_{m,o}}^{-\alpha/2}}{\sum_{k \in \mathbb{N}\setminus\{D_{m,o}\}} P_D h_k B_{D,k}^{-\alpha/2} \Xi_{D,k} + I_H}. \quad (25)$$

TABLE I
SYSTEM PARAMETERS

Symbol	r_D	r_H	β_H	P_D	P_H	M	α
Value	15 m	100 m	1	3 dBm	23 dBm	100	4

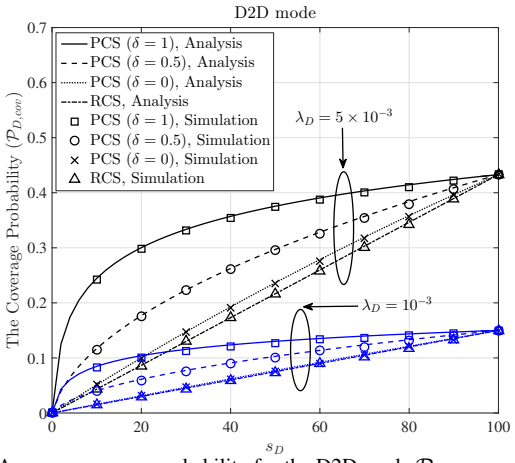

Fig. 1. Average coverage probability for the D2D mode $\mathcal{P}_{D,cov}$ as a function of s_D.

The expression for the coverage probability $\mathcal{P}_{D_m}$ in (8) is identified in the following theorem.

Theorem 3. *The coverage probability* $\mathcal{P}_{D_m}$ *in* (8) *is given by*

$$\mathcal{P}_{D_m} = \int_0^{r_D} \mathcal{L}_{I_H}\left(\frac{\gamma_{th} z^\alpha}{P_D}\right) \mathcal{L}_{I_{D_m}}\left(\frac{\gamma_{th} z^\alpha}{P_D}, z\right) f_{\|\mathbf{x}_{D_{m,o}}\|}(z)\, \mathrm{d}z, \tag{26}$$

$$f_{\|\mathbf{x}_{D_{m,o}}\|}(x) = 2\pi\eta_{D_m}\lambda_D x \exp\left(-\pi\eta_{D_m}\lambda_D x^2\right),$$

where $\mathcal{L}_{I_H}$ *and* $\mathcal{L}_{I_{D_m}}$ *are defined in* (13) *and* (18)*, respectively. When* $\Phi_H \sim PPP(\lambda_H)$*, the Laplace transform becomes* $\mathcal{L}_{I_H}(s) = \exp\left(-\frac{2\pi^2\lambda_H}{\alpha \sin\left(\frac{2\pi}{\alpha}\right)}(sP_H)^{2/\alpha}\right)$.

We skip the proof as (26) is obtained by proceeding precisely as in the proof of Theorem 2.

IV. Simulation Results

In this section, we illustrate numerical simulation results to validate our analysis. In Figs. 1-3, the lines and symbols are used to indicate the analytical and simulated results, respectively. Unless otherwise stated, we use the network parameters listed in Table I.

The average coverage probability $\mathcal{P}_{D,cov}$ in (10) is examined in Fig. 1 when $\gamma_{th} = -5$ dB, $\lambda_H = 5 \times 10^{-4}$ and $\Phi_H \sim GPP(\lambda_H, 1)$. Since the intensity of the D2D transmitters having the accessed content grows as λ_D and s_D become bigger, $\mathcal{P}_{D,cov}$ decreases as λ_D and s_D get smaller. Also, an increase in δ leads to a growth of $\{\eta_{D_m}\}$, and therefore $\mathcal{P}_{D,cov}$ is an increasing function of δ. Moreover, by comparing the cases "PCS ($\delta = 0$)" and "RCS", we can infer that a higher $\mathcal{P}_{D,cov}$ can be achieved by employing the PCS even when the content popularity follows the uniform distribution.

Figs. 2 and 3 present the coverage probability for the CH mode when $\lambda_D = 10^{-3}$ and $\gamma_{th} = -5$ dB. In Fig. 2, we plot the coverage probability $\mathcal{P}_{H_m}$ in (20) for various values of η_{H_m}. As λ_H and η_{H_m} grow, the probability that there exist CHs caching the requested content becomes larger

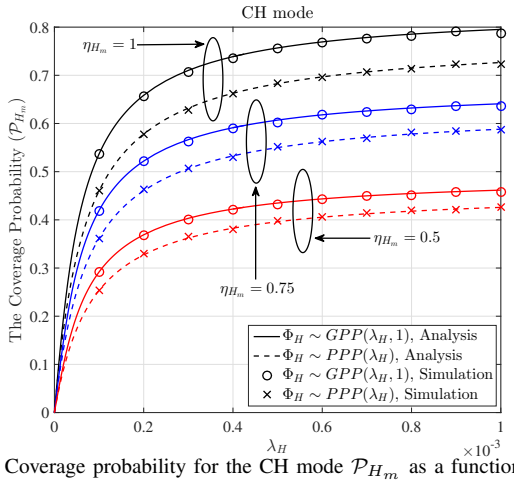

Fig. 2. Coverage probability for the CH mode $\mathcal{P}_{H_m}$ as a function of λ_H.

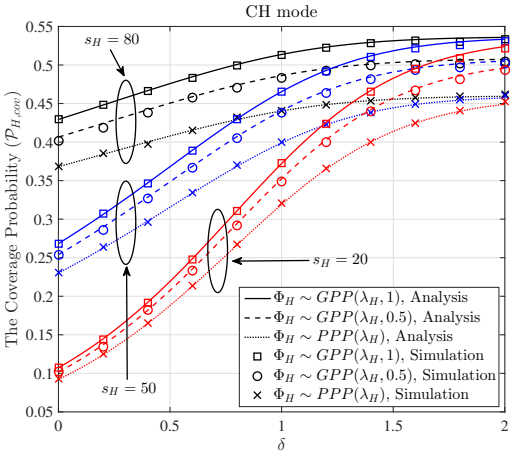

Fig. 3. Average coverage probability for the CH mode $\mathcal{P}_{H,cov}$ as a function of δ.

and the contact distance decreases, and hence $\mathcal{P}_{H_m}$ is an increasing function of λ_H and η_{H_m}. We remark that the interference from the CHs gets bigger as λ_H increases. From the observation that $\mathcal{P}_{H_m}$ increases with λ_H, we deduce that the impact of the contact distance is more pronounced than that of the interference. In addition, since the contact distance gets smaller if there exists repulsion among the locations of the CHs, $\mathcal{P}_{H_m}$ is larger when Φ_H follows a β-GPP than that when Φ_H follows a PPP.

Fig. 3 evaluates the average coverage probability for the CH mode $\mathcal{P}_{H,cov}$ in (11) for the networks where $\lambda_H = 10^{-4}$ and the PCS strategy is employed. Since increases in s_H and δ lead to a growth of the intensity of Φ_{H_m}, $\mathcal{P}_{H,cov}$ decays as s_H and δ become lower. As expected, $\mathcal{P}_{H,cov}$ increases as β_H goes to one. It is shown that $\mathcal{P}_{H,cov}$ is sensitive to δ when s_H is small. Also, the coverage probabilities with different values of s_H converge as δ increases since a small number of contents are frequently requested by users when δ is large.

V. Conclusion

In this paper, we have studied WCHNs where the locations of D2D transmitters and CHs are modeled by a PPP and a β-GPP, respectively. We have considered two types of access modes, namely D2D and CH modes and analyzed the coverage probabilities for the two modes. Numerical simulations have verified the accuracy of our analytical results.

APPENDIX A
PROOF OF THEOREM 1

We begin by defining a sequence of discrete random variables $\{\epsilon_{H,i}\}_{i\in\mathbb{N}}$ which are independent marks of Φ_H such that $\epsilon_{H,i}\in\{0,1\}$ and $\mathbb{P}(\epsilon_{H,i}=1)=\eta_{H_m}$. Here, $\{\epsilon_{H,i}=1\}$ and $\{\epsilon_{H,i}=0\}$ are the events wherein the CH at $\mathbf{x}_i$ has the content c_m and does not have it, respectively. For any $i\in\mathbb{N}$, we set

$$I_i := \bigcap_{k\in\mathbb{N}\setminus\{i\}} \big\{B_{H,k}\geq B_{H,i} \text{ or } \epsilon_{H,k}=0 \text{ or } \Xi_{H,k}=0\big\},$$

as well as $J_i := I_i\cap\{\epsilon_{H,i}=1\}\cap\{\Xi_{H,i}=1\}$, and it is easy to check that the events $\{J_i\}_{i\in\mathbb{N}}$ are disjoint almost surely. Additionally, on the event J_i we have $\|\mathbf{x}_{H_{m,o}}\|^2 = B_{H,i}$. Consequently, we have

$$\begin{aligned}
\mathcal{P}_{H_m} &\triangleq \mathbb{P}\big(\gamma_{H_m}\geq\gamma_{th}, \|\mathbf{x}_{H_{m,o}}\|\leq r_H\big)\\
&=\sum_{i=1}^{\infty}\mathbb{P}\big(\gamma_{H_m}\geq\gamma_{th},\ B_{H,i}\leq r_H^2,\ \epsilon_{H,i}=1,\ \Xi_{H,i}=1,\ I_i\big)\\
&=\sum_{i=1}^{\infty}\mathbb{P}\Bigg(g_i\geq\frac{\gamma_{th}B_{H,i}^{\alpha/2}}{P_H}\Bigg(\sum_{k\in\mathbb{N}\setminus\{i\}}P_Hg_kB_{H,k}^{-\alpha/2}\Xi_{H,k}+I_D\Bigg),\\
&\qquad B_{H,i}\leq r_H^2,\ I_i\Bigg)\mathbb{P}(\epsilon_{H,i}=1,\ \Xi_{H,i}=1)\\
&=\eta_{H_m}\beta_H\sum_{i=1}^{\infty}\mathbb{E}\Bigg[\exp\Bigg(-\frac{\gamma_{th}B_{H,i}^{\alpha/2}}{P_H}\\
&\quad\times\Bigg(\sum_{k\in\mathbb{N}\setminus\{i\}}P_Hg_kB_{H,k}^{-\alpha/2}\Xi_{H,k}+I_D\Bigg)\Bigg)\mathbb{1}_{\left\{B_{H,i}\leq r_H^2,\ I_i\right\}}\Bigg]\\
&=\eta_{H_m}\beta_H\sum_{i=1}^{\infty}\mathbb{E}\Bigg[\mathcal{L}_{I_D}\Bigg(\frac{\gamma_{th}B_{H,i}^{\alpha/2}}{P_H}\Bigg)\\
&\quad\times\prod_{k\in\mathbb{N}\setminus\{i\}}\exp\left(-\gamma_{th}B_{H,i}^{\alpha/2}g_kB_{H,k}^{-\alpha/2}\Xi_{H,k}\right)\mathbb{1}_{\left\{B_{H,i}\leq r_H^2,\ I_i\right\}}\Bigg]\\
&=\eta_{H_m}\beta_H\sum_{i=1}^{\infty}\mathbb{E}\Bigg[\mathcal{L}_{I_D}\left(\frac{\gamma_{th}B_{H,i}^{\alpha/2}}{P_H}\right)\mathbb{1}_{\left\{B_{H,i}\leq r_H^2\right\}}\\
&\quad\times\prod_{k\in\mathbb{N}\setminus\{i\}}\Bigg[\frac{1}{1+\gamma_{th}B_{H,i}^{\alpha/2}B_{H,k}^{-\alpha/2}\Xi_{H,k}}\\
&\qquad\times\mathbb{1}_{\left\{B_{H,k}\geq B_{H,i}\text{ or }\epsilon_{H,k}=0\text{ or }\Xi_{H,k}=0\right\}}\Bigg]\Bigg]\\
&=\eta_{H_m}\beta_H\sum_{i=1}^{\infty}\mathbb{E}\Bigg[\mathcal{L}_{I_D}\left(\frac{\gamma_{th}B_{H,i}^{\alpha/2}}{P_H}\right)\mathbb{1}_{\left\{B_{H,i}\leq r_H^2\right\}}\prod_{k\in\mathbb{N}\setminus\{i\}}\\
&\quad\times\left[1-\beta_H+\frac{\beta_H}{1+\gamma_{th}B_{H,i}^{\alpha/2}B_{H,k}^{-\alpha/2}}\mathbb{1}_{\left\{B_{H,k}\geq B_{H,i}\text{ or }\epsilon_{H,k}=0\right\}}\right]\Bigg].
\end{aligned}\tag{27}$$

We remark that $\mathbb{1}_{\{B_{H,k}\geq B_{H,i}\text{ or }\epsilon_{H,i}=0\}} = \mathbb{1}_{\{\epsilon_{H,i}=0\}} + \mathbb{1}_{\{B_{H,k}\geq B_{H,i}\text{ and }\epsilon_{H,i}=1\}}$, and therefore $\mathcal{P}_{H_m}$ in (27) is computed as

$$\begin{aligned}
\mathcal{P}_{H_m} &= \eta_{H_m}\beta_H\sum_{i=1}^{\infty}\mathbb{E}\Bigg[\mathcal{L}_{I_D}\left(\frac{\gamma_{th}B_{H,i}^{\alpha/2}}{P_H}\right)\mathbb{1}_{\left\{B_{H,i}\leq r_H^2\right\}}\\
&\quad\times\prod_{k\in\mathbb{N}\setminus\{i\}}\Bigg[1-\beta_H+\frac{\eta_{H_m}\beta_H}{1+\gamma_{th}B_{H,i}^{\alpha/2}B_{H,k}^{-\alpha/2}}\mathbb{1}_{\left\{B_{H,k}\geq B_{H,i}\right\}}\\
&\quad+\frac{(1-\eta_{H_m})\beta_H}{1+\gamma_{th}B_{H,i}^{\alpha/2}B_{H,k}^{-\alpha/2}}\Bigg]\Bigg]\\
&=\eta_{H_m}\beta_H\sum_{i=1}^{\infty}\int_0^{r_H^2}\mathcal{L}_{I_D}\left(\frac{\gamma_{th}u^{\alpha/2}}{P_H}\right)f_{B_{H,i}}(u)\\
&\quad\times\prod_{k\in\mathbb{N}\setminus\{i\}}\Bigg(1-\beta_H+\int_u^{\infty}\frac{\eta_{H_m}\beta_H}{1+\gamma_{th}u^{\alpha/2}x^{-\alpha/2}}f_{B_{H,k}}(x)\,\mathrm{d}x\\
&\quad+\int_0^{\infty}\frac{(1-\eta_{H_m})\,\beta_H}{1+\gamma_{th}u^{\alpha/2}x^{-\alpha/2}}f_{B_{H,k}}(x)\,\mathrm{d}x\Bigg)\mathrm{d}u\\
&=2\eta_{H_m}\beta_H\sum_{i=1}^{\infty}\int_0^{r_H}\mathcal{L}_{I_D}\left(\frac{\gamma_{th}z^{\alpha}}{P_H}\right)f_{B_{H,i}}(z^2)\\
&\quad\times\prod_{k\in\mathbb{N}\setminus\{i\}}\Bigg(1-\beta_H+\int_{z^2}^{\infty}\frac{\eta_{H_m}\beta_H}{1+\gamma_{th}z^{\alpha}x^{-\alpha/2}}f_{B_{H,k}}(x)\,\mathrm{d}x\\
&\quad+\int_0^{\infty}\frac{(1-\eta_{H_m})\,\beta_H}{1+\gamma_{th}z^{\alpha}x^{-\alpha/2}}f_{B_{H,k}}(x)\,\mathrm{d}x\Bigg)z\,\mathrm{d}z.
\end{aligned}\tag{28}$$

Here, by (12) and a change of variable, the inner integral terms in (28) can be rewritten as

$$\begin{aligned}
&\int_{z^2}^{\infty}\frac{\eta_{H_m}\beta_H}{1+\gamma_{th}z^{\alpha}x^{-\alpha/2}}f_{B_{H,k}}(x)\,\mathrm{d}x \qquad (29)\\
&=\int_{\pi\lambda_Hz^2/\beta_H}^{\infty}\frac{\eta_{H_m}\beta_H\nu^{k-1}\exp(-\nu)}{\Gamma(k)\left(1+\gamma_{th}\left(\frac{\pi\lambda_Hz^2}{\beta_H}\right)^{\alpha/2}\nu^{-\alpha/2}\right)}\,\mathrm{d}\nu,\\
&\int_0^{\infty}\frac{(1-\eta_{H_m})\,\beta_H}{1+\gamma_{th}z^{\alpha}x^{-\alpha/2}}f_{B_{H,k}}(x)\,\mathrm{d}x \qquad (30)\\
&=\int_0^{\infty}\frac{(1-\eta_{H_m})\,\beta_H\nu^{k-1}\exp(-\nu)}{\Gamma(k)\left(1+\gamma_{th}\left(\frac{\pi\lambda_Hz^2}{\beta_H}\right)^{\alpha/2}\nu^{-\alpha/2}\right)}\,\mathrm{d}\nu.
\end{aligned}$$

By plugging (29) and (30) into (28), we obtain the result in (20).

APPENDIX B
PROOF OF THEOREM 2

The aim of the proof is to compute the limit of (20) as β_H goes to zero. First, note that for any $x>0$ we have

$$\begin{aligned}
0&\leq\int_x^{\infty}\frac{\eta_{H_m}\beta_H\nu^{k-1}\exp(-\nu)}{\Gamma(k)\left(1+\gamma_{th}x^{\alpha/2}\nu^{-\alpha/2}\right)}\,\mathrm{d}\nu \qquad (31)\\
&\leq\int_0^{\infty}\frac{\eta_{H_m}\beta_H\nu^{k-1}\exp(-\nu)}{\Gamma(k)}\,\mathrm{d}\nu=\eta_{H_m}\beta_H,
\end{aligned}$$

and similarly

$$0\leq\int_0^{\infty}\frac{(1-\eta_{H_m})\beta_H\nu^{i-1}\exp(-\nu)}{\Gamma(i)\left(1+\gamma_{th}x^{\alpha/2}\nu^{-\alpha/2}\right)}\,\mathrm{d}\nu\leq(1-\eta_{H_m})\beta_H. \tag{32}$$

Thus, taking $x=\pi\lambda_Hz^2/\beta_H$ we obtain

$$1\leq\exp\left(-\frac{\pi\lambda_Hz^2}{\beta_H}\right)\Upsilon_{H_m}\left(\frac{\pi\lambda_Hz^2}{\beta_H}\right)\leq(1-\beta_H)^{-1}, \tag{33}$$

which implies

$$\exp\left(-\frac{\pi\lambda_Hz^2}{\beta_H}\right)\Upsilon_{H_m}\left(\frac{\pi\lambda_Hz^2}{\beta_H}\right)\xrightarrow[\beta_H\to0]{}1. \tag{34}$$

Second, let us fix $\varepsilon>0$ and $x>0$. By (31) and (32), for any $k\geq1$ we have

$$\begin{aligned}
0\leq\beta_H&-\int_{x/\beta_H}^{\infty}\frac{\eta_{H_m}\beta_H\nu^{k-1}\exp(-\nu)}{\Gamma(k)\left(1+\gamma_{th}x^{\alpha/2}(\nu\beta_H)^{-\alpha/2}\right)}\,\mathrm{d}\nu \qquad (35)\\
&-\int_0^{\infty}\frac{(1-\eta_{H_m})\beta_H\nu^{k-1}\exp(-\nu)}{\Gamma(k)\left(1+\gamma_{th}x^{\alpha/2}(\nu\beta_H)^{-\alpha/2}\right)}\,\mathrm{d}\nu\leq\beta_H,
\end{aligned}$$

and additionally we note that

$$\begin{aligned}\beta_H &- \int_{x/\beta_H}^{\infty} \frac{\eta_{H_m}\beta_H\nu^{k-1}\exp(-\nu)}{\Gamma(k)\,(1+\gamma_{th}x^{\alpha/2}(\nu\beta_H)^{-\alpha/2})}\,\mathrm{d}\nu \\ &- \int_0^{\infty} \frac{(1-\eta_{H_m})\beta_H\nu^{k-1}\exp(-\nu)}{\Gamma(k)\,(1+\gamma_{th}x^{\alpha/2}(\nu\beta_H)^{-\alpha/2})}\,\mathrm{d}\nu \\ &= \int_0^{x/\beta_H} \frac{\eta_{H_m}\beta_H\nu^{k-1}\exp(-\nu)}{\Gamma(k)\,(1+\gamma_{th}x^{\alpha/2}(\nu\beta_H)^{-\alpha/2})}\,\mathrm{d}\nu \\ &+ \int_0^{\infty} \frac{\beta_H\nu^{k-1}\exp(-\nu)}{\Gamma(k)\,(1+(\nu\beta_H)^{\alpha/2}x^{-\alpha/2}/\gamma_{th})}\,\mathrm{d}\nu. \end{aligned} \tag{36}$$

For x sufficiently small, the inequalities $-(1+\varepsilon)x \le \ln(1-x) \le -x$ hold, and therefore by (35) and (36), for β_H sufficiently small we have

$$\begin{aligned}&-(1+\varepsilon)\bigg(\int_0^{x/\beta_H} \frac{\eta_{H_m}\beta_H\nu^{k-1}\exp(-\nu)}{\Gamma(k)\,(1+\gamma_{th}x^{\alpha/2}(\nu\beta_H)^{-\alpha/2})}\,\mathrm{d}\nu \\ &\quad+\int_0^{\infty} \frac{\beta_H\nu^{k-1}\exp(-\nu)}{\Gamma(k)\,(1+(\nu\beta_H)^{\alpha/2}x^{-\alpha/2}/\gamma_{th})}\,\mathrm{d}\nu\bigg) \\ &\le \ln\bigg(1-\beta_H+\int_{x/\beta_H}^{\infty} \frac{\eta_{H_m}\beta_H\nu^{k-1}\exp(-\nu)}{\Gamma(k)\,(1+\gamma_{th}x^{\alpha/2}(\nu\beta_H)^{-\alpha/2})}\,\mathrm{d}\nu \\ &\quad+\int_0^{\infty} \frac{(1-\eta_{H_m})\beta_H\nu^{k-1}\exp(-\nu)}{\Gamma(k)\,(1+\gamma_{th}x^{\alpha/2}(\nu\beta_H)^{-\alpha/2})}\,\mathrm{d}\nu\bigg) \\ &\le -\int_0^{x/\beta_H} \frac{\eta_{H_m}\beta_H\nu^{k-1}\exp(-\nu)}{\Gamma(k)\,(1+\gamma_{th}x^{\alpha/2}(\nu\beta_H)^{-\alpha/2})}\,\mathrm{d}\nu \\ &\quad-\int_0^{\infty} \frac{\beta_H\nu^{k-1}\exp(-\nu)}{\Gamma(k)\,(1+(\nu\beta_H)^{\alpha/2}x^{-\alpha/2}/\gamma_{th})}\,\mathrm{d}\nu,\end{aligned}$$

for all $k \ge 1$. We deduce from the above inequalities that for β_H sufficiently small the following holds:

$$\begin{aligned}&\exp\bigg(-(1+\varepsilon)\bigg(\int_0^{x/\beta_H} \frac{\eta_{H_m}\beta_H\,\mathrm{d}\nu}{1+\gamma_{th}x^{\alpha/2}(\nu\beta_H)^{-\alpha/2}} \\ &\quad+\int_0^{\infty} \frac{\beta_H\,\mathrm{d}\nu}{1+(\nu\beta_H)^{\alpha/2}x^{-\alpha/2}/\gamma_{th}}\bigg)\bigg) \le \Delta_{H_m}\left(\frac{x}{\beta_H}\right) \\ &\le \exp\bigg(-\int_0^{x/\beta_H} \frac{\eta_{H_m}\beta_H}{1+\gamma_{th}x^{\alpha/2}(\nu\beta_H)^{-\alpha/2}}\,\mathrm{d}\nu \\ &\quad-\int_0^{\infty} \frac{\beta_H}{1+(\nu\beta_H)^{\alpha/2}x^{-\alpha/2}/\gamma_{th}}\,\mathrm{d}\nu\bigg),\end{aligned}$$

and so by change of variable,

$$\begin{aligned}&\exp\bigg(-(1+\varepsilon)\bigg(\int_0^{x} \frac{\eta_{H_m}\,\mathrm{d}y}{1+\gamma_{th}x^{\alpha/2}y^{-\alpha/2}} \\ &\quad+\int_0^{\infty} \frac{\mathrm{d}y}{1+y^{\alpha/2}x^{-\alpha/2}/\gamma_{th}}\bigg)\bigg) \le \Delta_{H_m}\left(\frac{x}{\beta_H}\right) \\ &\le \exp\bigg(-\int_0^{x} \frac{\eta_{H_m}\,\mathrm{d}y}{1+\gamma_{th}x^{\alpha/2}y^{-\alpha/2}} \\ &\quad-\int_0^{\infty} \frac{\mathrm{d}y}{1+y^{\alpha/2}x^{-\alpha/2}/\gamma_{th}}\bigg).\end{aligned} \tag{37}$$

Since the above is true for all $\varepsilon > 0$, we obtain

$$\begin{aligned}\Delta_{H_m}\left(\frac{x}{\beta_H}\right) &\xrightarrow[\beta_H\to 0]{} \exp\bigg(-\int_0^{x} \frac{\eta_{H_m}\,\mathrm{d}y}{1+\gamma_{th}x^{\alpha/2}y^{-\alpha/2}} \\ &\quad-\int_0^{\infty} \frac{\mathrm{d}y}{1+y^{\alpha/2}x^{-\alpha/2}/\gamma_{th}}\bigg) \\ &= \exp\bigg(-\eta_{H_m}x-\eta_{H_m}\int_x^{\infty} \frac{\mathrm{d}y}{1+y^{\alpha/2}x^{-\alpha/2}/\gamma_{th}} \\ &\quad-\int_0^{\infty} \frac{(1-\eta_{H_m})\,\mathrm{d}y}{1+y^{\alpha/2}x^{-\alpha/2}/\gamma_{th}}\bigg).\end{aligned}$$

By taking $x = \pi\lambda_H z^2$ in the above series of equations, we get

$$\Delta_{H_m}\left(\frac{\pi\lambda_H z^2}{\beta_H}\right) \xrightarrow[\beta_H\to 0]{} \exp(-\pi\eta_{H_m}\lambda_H z^2)\mathcal{L}_{I_{H_m}}\left(\frac{\gamma_{th}z^{\alpha}}{P_H}, z\right). \tag{38}$$

By the bounds given in (33) and (37) and the almost sure convergence proved in (34) and (38), one may apply the dominated convergence theorem to prove the convergence of (20) to (24) as β_H goes to zero.

REFERENCES

[1] Cisco, "Cisco visual networking index: Global mobile data traffic forecast update, 2016-2021," 2017.

[2] X. Wang, M. Chen, T. Taleb, A. Ksentini, and V. C. M. Leung, "Cache in the air: exploiting content caching and delivery techniques for 5G systems," *IEEE Commun. Mag.*, vol. 52, pp. 131–139, Feb. 2014.

[3] K. Shanmugam, N. Golrezaei, A. G. Dimakis, A. F. Molisch, and G. Caire, "Femtocaching: Wireless content delivery through distributed caching helpers," *IEEE Trans. Inf. Theory*, vol. 59, pp. 8402–8413, Dec. 2013.

[4] M. Ji, G. Caire, and A. F. Molisch, "Fundamental limits of caching in wireless D2D networks," *IEEE Trans. Inf. Theory*, vol. 62, pp. 849–869, Feb. 2016.

[5] S. Tamoor-ul-Hassan, M. Bennis, P. H. J. Nardelli, and M. Latva-aho, "Caching in wireless small cell networks: A storage-bandwidth tradeoff," *IEEE Commun. Lett.*, vol. 20, pp. 1175–1178, Jun. 2016.

[6] E. Baştuğ, M. Bennis, M. Kountouris, and M. Debbah, "Cache-enabled small cell networks: modeling and tradeoffs," *EURASIP J. Wireless Commun. Netw.*, vol. 41, pp. 1–11, Dec. 2015.

[7] D. Malak, M. Al-Shalash, and J. G. Andrews, "Optimizing content caching to maximize the density of successful receptions in device-to-device networking," *IEEE Trans. Commun.*, vol. 64, pp. 4365–4380, Oct. 2016.

[8] S. H. Chae and W. Choi, "Caching placement in stochastic wireless caching helper networks: Channel selection diversity via caching," *IEEE Trans. Wireless Commun.*, vol. 15, pp. 6626–6637, Oct. 2016.

[9] S. H. Chae, T. Q. S. Quek, and W. Choi, "Content placement for wireless cooperative caching helpers: A tradeoff between cooperative gain and content diversity gain," *IEEE Trans. Wireless Commun.*, vol. 16, pp. 6795–6807, Oct. 2017.

[10] A. Guo and M. Haenggi, "Spatial stochastic models and metrics for the structure of base stations in cellular networks," *IEEE Trans. Wireless Commun.*, vol. 12, pp. 5800–5812, Nov. 2013.

[11] L. Decreusefond, I. Flint, and A. Vergne, "Efficient simulation of the Ginibre point process," *Adv. Appl. Probab.*, vol. 52, pp. 1–21, Oct. 2015.

[12] H.-B. Kong, P. Wang, D. Niyato, and Y. Cheng, "Modeling and analysis of wireless sensor networks with/without energy harvesting using Ginibre point processes," *IEEE Trans. Wireless Commun.*, vol. 16, pp. 3700–3713, Jun. 2017.

[13] H. B. Kong, I. Flint, P. Wang, D. Niyato, and N. Privault, "Exact performance analysis of ambient RF energy harvesting wireless sensor networks with Ginibre point process," *IEEE J. Sel. Areas Commun.*, vol. 34, pp. 3769–3784, Dec. 2016.

[14] N. Deng, W. Zhou, and M. Haenggi, "The Ginibre point process as a model for wireless networks with repulsion," *IEEE Trans. Wireless Commun.*, vol. 14, pp. 107–121, Jan. 2015.

[15] I. Nakata and N. Miyoshi, "Spatial stochastic models for analysis of heterogeneous cellular networks with repulsively deployed base stations," *Performance Evaluation*, vol. 78, pp. 7–17, Aug. 2014.

[16] T. Shirai and Y. Takahashi, "Random point fields associated with certain Fredholm determinants I: Fermion, Poisson and boson point processes," *J. Functional Anal.*, vol. 205, pp. 414–463, Apr. 2003.

[17] A. Goldman, "The Palm measure and the Voronoi tessellation for the Ginibre process," *Ann. Appl. Probab.*, vol. 20, pp. 90–128, 2010.

[18] M. Zink, K. Suh, Y. Gu, and J. Kurose, "Characteristics of youtube network traffic at a campus network-measurements, models, and implications," *Comput. Netw.*, vol. 53, pp. 501–514, Mar. 2009.

[19] M. Haenggi, *Stochastic geometry for wireless networks*. Cambridge, U.K.: Cambridge Univ. Press, 2012.